

Fermi National Accelerator Laboratory

FERMILAB-Pub-90/244-A

December 1990

TELESCOPE SEARCH FOR MULTI-eV AXIONS

Matthew A. Bershadsky,^a M. Ted Ressel,^{a,b} and Michael S. Turner^{a,b,c}

^aDepartment of Astronomy & Astrophysics
The University of Chicago
Chicago, IL 60637-1433

^bNASA/Fermilab Astrophysics Center
Fermi National Accelerator Laboratory
Batavia, IL 60510-0500

^cDepartment of Physics
Enrico Fermi Institute
The University of Chicago
Chicago, IL 60637-1433

Abstract. An axion of mass 3 eV to 8 eV has a cosmological abundance of about 50 cm^{-3} . Such relic axions reside in rich clusters of galaxies. Their decays to two photons produce a line at a wavelength $\lambda_a \sim 3100 \text{ \AA} - 8300 \text{ \AA}$ whose width $\Delta\lambda/\lambda \sim 10^{-2}$. We have searched unsuccessfully for such a feature in the intergalactic light of three rich clusters, closing this "window," and leaving open only the window from 10^{-6} eV to 10^{-3} eV . Our flux limits are also of relevance to other relics whose decays produce mono-energetic photons.



Introduction. Peccei–Quinn (PQ) symmetry and the axion are a compelling and modest extension of the standard model: PQ symmetry provides the most attractive solution to the strong- CP problem.¹ Moreover, the axion arises in supersymmetric theories and superstring theories. The coupling strength of the axion to ordinary matter is inversely proportional to the PQ symmetry breaking scale f_a which also determines the axion mass:

$$m_a \simeq \frac{\sqrt{z}}{1+z} \frac{f_\pi m_\pi}{(f_a/N)} \simeq \frac{0.62 \text{ eV}}{(f_a/N)/10^7 \text{ GeV}}; \quad (1)$$

$z \simeq 0.56$ is the ratio of up to down quark masses, f_π and m_π are the pion decay constant and mass, and N is the color anomaly of PQ symmetry. At present there is little theoretical guidance as to the axion mass, with plausible values ranging from about 10^{-11} eV to 200 keV! However, laboratory experiments and a host of astrophysical and cosmological arguments have narrowed this to two “windows:” 10^{-6} eV 10^{-3} eV; and 3 eV to 8 eV (hadronic axions only).² In the first window axions can close the Universe; several cosmic axion searches have been carried out, and a new, more sensitive search is planned.³

Axions of mass 3 eV to 8 eV come into thermal equilibrium in the early Universe, decouple when the temperature was about 100 MeV, and should today have a abundance of about 50 cm^{-3} , comparable to that of neutrinos.⁴ Their contribution to the critical density is small, $\Omega_a \simeq m_a/(49h_{50}^2 \text{ eV})$ (the Hubble constant $H_0 = 50h_{50} \text{ km s}^{-1} \text{ Mpc}^{-1}$). Although multi-eV axions cannot comprise the ubiquitous dark matter, they might be detected through their decay to two photons.^{4,5} The axion mean lifetime is

$$\tau(a \rightarrow 2\gamma) \simeq 6.8 \times 10^{24} \zeta^{-2} (m_a/\text{eV})^{-5} \text{ sec}, \quad (2)$$

where $\zeta \equiv [E/N - 2(z+4)/3(z+1)]/0.72 \simeq (E/N - 1.95)/0.72$ and E is the electromagnetic anomaly of PQ symmetry. In the simplest axion models, $E/N = 8/3$ and $\zeta = 1$.

Relic thermal axions will, in accord with the equivalence principle, fall with baryons (and any other particles) into the various potential wells that develop in the Universe, and will be found in extended structures around galaxies (halos) and in clusters of galaxies, as they cannot dissipate energy and condense further. Their decays will produce a line at wavelength $\lambda_a \simeq 24800 \text{ \AA}/(m_a/\text{eV})$, which is Doppler-broadened by the velocities that axions have in these objects, and for distant objects the line is also red shifted: $\lambda = (1+z)\lambda_a$. The most promising case for detection is that of cluster axions where the expected line intensity is $I_a \sim 10^{-17} \zeta^2 (m_a/3 \text{ eV})^7 \text{ erg cm}^{-2} \text{ arcsec}^{-2} \text{ \AA}^{-1} \text{ s}^{-1}$.⁴ The background with which this must compete is the “night sky.” At a ground-based observatory the night sky is dominated by the glow of the atmosphere, includes many strong lines, and has a continuum intensity of roughly $10^{-17} \text{ erg cm}^{-2} \text{ arcsec}^{-2} \text{ \AA}^{-1} \text{ s}^{-1}$.⁶ In this *Letter* we report the results of a search for an intracluster axion line carried out at Kitt Peak National Observatory (KPNO) last May. We observed three rich clusters and found no evidence for an

axion line, and are able to rule out an axion of mass in the range $3.2 \text{ eV} \max[1, (\zeta/0.5)^{-2/7}]$ to 7.8 eV , effectively closing this “window” unless $\zeta \ll 1$.⁷

Observing strategy. We selected three well studied, rich clusters of galaxies:⁸ Abell 1413 ($z = 0.143$), 2218 ($z = 0.171$), and 2256 ($z = 0.0601$). The red shifts of these clusters are large enough so that the angular sizes of the clusters are comparable to our field of view (5 arcmin), and small enough so that the axion line is not shifted too far into the red or diminished too much in strength. Each of the clusters has been the subject of extensive dynamical studies and x-ray observations, which aids in modeling the axion line expected.

Our strategy for dealing with the night sky is simple. Since axions share the same potential well as the galaxies and x-ray emitting gas, the axion-line intensity should decrease going from cluster center outward. We take a spectrum from near the cluster center and subtract from it a spectrum from the outer reaches of the cluster. In principle, this procedure should completely remove the night sky with minimal effect to the axion line. Since the night sky brightness varies both spatially and temporally, it is important that the “off cluster” data and the “on cluster” data be taken as close in space and time as possible. Even so, the bright emission lines and the OH bands in the red are still troublesome. Fig. 1 is typical of the subtracted spectra we obtained. Subtraction works quite well except where there are bright night-sky lines, and sensitivities of a few % of the continuum night-sky brightness are typical. Because the axion line is red shifted by different amounts in the different clusters while the night-sky lines remain fixed, the spectral regions where the subtraction is poor correspond to different axion masses in the different clusters.

How can we recognize an axion line? First, the line should be seen at different wavelengths in the different clusters, because the red shifts of the clusters are different. Next, the line should have the predicted strength and should be Doppler-broadened to a gaussian of width $\Delta\lambda/\lambda = 2\sqrt{\ln 4}\sigma/c$, where σ is the one-dimensional velocity dispersion of the cluster. Finally, since cluster axions behave as a gas of collisionless particles they should have a density profile described by an isothermal sphere,⁹ and the spatial variation of the line strength provides another check. While it is impossible to make the case with certainty; e.g., an intracluster atomic-emission line could satisfy all these criteria, we have enough redundancy to make a strong case.

In modeling the axion line we used the analytic King model approximation^{9,10} to an isothermal sphere, which has a density run $\rho(r) = \rho_c / (1 + r^2/a^2)^{3/2}$, where a is the core radius, r is the radial distance from cluster center, and the central density is $\rho_c = 9\sigma^2/4\pi Ga^2$. Relic axions only make up a fraction of the cluster mass. In objects that have not undergone significant dissipation—including clusters—the ratio of the axion-to-baryon mass densities should remain constant. This means that the axion mass density in the

cluster should be related to that of baryons: $\rho_a \simeq (\Omega_a/\Omega_B)\rho_B$. However, the mass of the cluster may not be primarily baryonic—it could be particle dark matter. Taking this into account, and assuming that particle dark matter contributes at most closure density, we can relate the axion mass density to the cluster mass density: $\rho_a \simeq \rho(\Omega_a \rightarrow \Omega_a/\Omega_B)$. Combining this with the well known bound from nucleosynthesis:¹¹ $0.04 \lesssim \Omega_B h_{50}^2 \lesssim 0.10$, we find $\rho_a = \Omega_a(1 \rightarrow 25h_{50}^2)\rho$. We will use the most conservative assumption, $\rho_a = \Omega_a\rho$.

Having related ρ_a to the cluster density ρ , it is now straightforward to write down the predicted axion-line intensity in the *cluster rest frame*:

$$I_a(R, \lambda) = \frac{\Sigma_a(R)c^3}{4\pi\sqrt{2\pi}\sigma\lambda_a\tau_a} \exp\left(\frac{-(\lambda - \lambda_a)^2 c^2}{\lambda_a^2 2\sigma^2}\right), \quad (3a)$$

$$= 1.0 \times 10^{-20} \left(\frac{m_a}{\text{eV}}\right)^7 \left(\frac{\sigma_3}{h_{50}a_{250}}\right) \zeta^2 \exp\left(\frac{-(\lambda - \lambda_a)^2 c^2}{\lambda_a^2 2\sigma^2}\right) / (1 + R^2/a^2), \quad (3b)$$

in units of $\text{erg cm}^{-2} \text{arcsec}^{-2} \text{\AA}^{-1} \text{s}^{-1}$, where $\Sigma_a = 9\sigma^2\Omega_a/2\pi Ga^2(1 + R^2/a^2)$ is the axion surface density, R is the projected radial distance from cluster center, $a = a_{250} 250 \text{ kpc}$, and $\sigma = \sigma_3 1000 \text{ km s}^{-1}$ (see Table 1). In our rest frame the line is red shifted by $(1+z)$ and I_a is “dimmed” by $(1+z)^{-4}$. The key features of the axion line are: extreme sensitivity to the axion mass ($\propto m_a^7$); varies as R^{-2} for $R \gg a$; and axion-model dependence ($\propto \zeta^2$).

The data. Our observations were made on the nights of 24 and 25 May 1990 at KPNO using the 2.1 meter telescope and Gold Camera CCD spectrograph at a spectral resolution of about 10\AA (the axion-line width is about $250 \text{\AA} \cdot \text{eV}/m_a$). The incoming light passes through a $5'$ by $2''.5$ slit onto the grating of the spectrograph, which disperses the one-dimensional slit image onto 480×800 pixels of the CCD. Each CCD exposure is a two-dimensional image: spatial position along the slit (480 pixels; $0''.78/\text{pixel}$) by spectral position (800 pixels; $4.6 \text{\AA}/\text{pixel}$). To minimize the effects of read noise we binned the pixels in the spatial dimension by three's, so that each CCD exposure contains 160 independent spectra (along the slit). On the first night we took multiple exposures of all three clusters in the wavelength range $4762 \text{\AA} - 8441 \text{\AA}$ (axion masses from 6.1 eV to 3.2 eV) by “walking” the slit from cluster core outward along an E-W axis. We did this to cover a large enough portion of the cluster to determine the spatial profile of the axion line (spatial coverage of 3 to 10 core radii). On the second night, we changed the grating to cover the spectral range from $3737 \text{\AA} - 7606 \text{\AA}$ (axion masses from 7.8 eV to 3.7 eV), and took single exposures of the two smaller clusters. Our exposure times ranged from 30 to 75 minutes (see Table 1).

The data were reduced using the KPNO Image Reduction and Analysis Facility software (IRAF). The CCD bias was subtracted and spatial variations in the pixel response and illumination were removed by “dividing” the CCD images by dome and sky flats taken

earlier in the evening. Exposures of a He-Ne-Ar lamp were used to provide wavelength calibration. Finally, we used observations of the KPNO standard star (Wolf 1346) to obtain absolute flux calibrations.

In Figs. 1 and 2 we show the “on cluster” spectrum (30 spatial pixels near cluster center) minus the “off cluster” spectrum (30 spatial pixels about five core radii from center) for A2218 and A2256, and in Fig. 2 we have artificially introduced the line expected from a 3.2 eV axion. There is no obvious candidate line in either “on – off” spectrum (or in any of our “on – off” spectra), even as weak as that expected for a 3.2 eV line. Since $I_a \propto m_a^7$, the line expected for $m_a > 3.2$ eV should be much more prominent. On this basis, we exclude the existence of an axion line for masses from 3.2 eV to 7.8 eV, the full range of our search.

Given the uncertainties in predicting the strength of the axion line and the fact that our search may have other relevance, we felt it useful to derive a quantitative flux limit to the existence of any intracluster line. To do so, we performed a cross-correlation analysis between the various “on – off” cluster spectra.¹² The basic idea is simple: While the wavelength of the would-be line is unknown, a line intrinsic to the cluster will appear at different wavelengths in different clusters: $\lambda_i = (1 + z_i)\lambda_a$, and will lead to a positive peak in the cross-correlation function of the “on – off” spectra for any two clusters,

$$\xi(l) = \frac{\int I_1(x)I_2(x+l)dx}{(\int I_1^2 dx \int I_2^2 dx)^{1/2}} = \frac{\int I_1(k)^* I_2(k) \exp(-ikl)dk}{(\int I_1(k)^2 dk \int I_2(k)^2 dk)^{1/2}}, \quad (4)$$

at “lag” $l = \ln[(1 + z_2)/(1 + z_1)]$, where the variable $x = \ln(\lambda)$. Moreover, the height and width of the peak in $\xi(l)$ are directly related to the intensity and width of the intracluster line. A statistically significant peak at the correct lag and of proper width would provide strong evidence for an intracluster emission line (albeit, unknown wavelength).

To assess the statistical significance of a peak, one has to know the distribution of “false” peaks due to “noise.” In computing $\xi(l)$ we have eliminated all prominent features in the “on – off” spectra that are obviously associated with cosmic-ray hits or poor night-sky line subtractions to justify arguing that the distribution of the remaining (random-noise) peaks in $\xi(l)$ is gaussian. It then follows that the distribution of positive peak heights h is $P(> h) = \int_h^\infty \exp(-h^2/4\sigma_\xi^2)dh/\sqrt{\pi}\sigma_\xi$, where σ_ξ is the rms of $\xi(l)$.

We find no obvious peak in the cross-correlation of A2218 and A2256 at the correct lag, $\exp(l) = (1 + z_{2218})/(1 + z_{2256})$. The nearest peak occurs at a lag of about 15% smaller, and has a height that corresponds to a point in the noise-peak distribution where there is a 39% probability of having a peak of this height or larger. To set flux limits we artificially introduced a line into the “on – off” spectra and cross correlated these spectra individually with a noiseless “template” containing the expected axion line. We then adjusted the strength of the artificial line until the height of the cross-correlation peak was

such that there is only a 5% probability for a peak of this height or larger arising due to gaussian noise. That gives us a “ 2σ ” limit to the flux from any undetected intracluster line. Our 2σ flux limits (in units of $\text{erg cm}^{-2} \text{arcsec}^{-2} \text{\AA}^{-1} \text{s}^{-1}$) are: 1.35×10^{-18} , 8.0×10^{-19} , 4.6×10^{-19} , 6.6×10^{-19} , 5.9×10^{-19} , and 1.3×10^{-18} for axion masses of 3.5 eV, 4.0 eV, 4.5 eV, 5.0 eV, 6.0 eV, and 7.5 eV respectively.

Concluding remarks. In this *Letter* we have described the results of an unsuccessful telescope search for line radiation from the decay of cluster axions of mass 3.2 eV to 7.8 eV. While our results seem to close this window, we remind the reader that there are astrophysical and particle physics uncertainties in the predicted line strength. We have been very conservative in treating the astrophysical uncertainties, perhaps by even a factor of 30. A remaining worry is that axions could be more smoothly distributed than we have assumed so that in our “on – off” subtractions we have eliminated the axion line too. To address this we have subtracted the “on cluster” spectrum of A2218 from that of A2256; the axion signature is one negative line and one positive line displaced in wavelength by a factor of $(1 + z_{2218})/(1 + z_{2256})$. While the night-sky subtraction was typically a factor of four worse, it was adequate and we found no evidence for the axion signature.

The most significant axion model dependence is embodied in ζ . In the simplest axion models $\zeta = 1$; but if E/N is very close to two, ζ could be very small. Since $I_a \propto \zeta^2 m_a^7$ the ζ dependence is only of concern for small axion masses. Using our line-flux limits, we can estimate the ζ dependence of our excluded mass region: 3.2 eV $\max[1, (\zeta/0.5)^{-2/7}]$ to 7.8 eV. Unless ζ is very small our search has closed the multi-eV window.

Finally, we note that our flux limits are applicable to any relic species that resides in clusters and whose decays produce mono-energetic photons of energy 1.6 eV to 3.9 eV. The expected line strength can be generalized to another relic X by multiplying I_a by a factor of $(n_\gamma/2)(\Omega_X/\Omega_a)(\tau_a/\tau_X)$, where $n_\gamma = 1$ or 2 is the number of photons produced per decay. For example, as applied to the decay of relic neutrinos, $\nu \rightarrow \nu' + \gamma$,

$$I_\nu(R, \lambda) = 4.8 \times 10^{-20} \left(\frac{m_\nu}{\text{eV}}\right)^2 \left(\frac{\sigma_3}{h_{50} a_{250}}\right) \left(\frac{10^{24} \text{ sec}}{\tau_\nu/B_\gamma}\right) \exp\left(\frac{-(\lambda - \lambda_a)^2 c^2}{\lambda_a^2 2\sigma^2}\right) / (1 + R^2/a^2), \quad (5)$$

in units of $\text{erg cm}^{-2} \text{arcsec}^{-2} \text{\AA}^{-1} \text{s}^{-1}$ where $\tau_{24} = \tau/10^{24} \text{ yr}$ and B_γ is the radiative branching ratio. Our previous 2σ flux limits then imply that: $\tau_{24}/B_\gamma > 0.40, 0.90, 1.94, 1.67, 2.7,$ and 1.9 for masses of 3.5 eV, 4.0 eV, 4.5 eV, 5.0 eV, 6.0 eV, and 7.5 eV.¹³

This work was supported by the NASA (at Fermilab through grant NAGW-1340 and at Chicago through MAB’s and MTR’s GSRP Fellowships), the DOE (at Chicago and Fermilab), and by the NSF (at Chicago). We thank Alan Dressler, Brian Yanny, Mike

Fitzpatrick, Rich Kron, and the staff at KPNO for valuable comments and assistance.

References

1. R.D. Peccei and H.R. Quinn, *Phys. Rev. Lett.* 38, 1440 (1977); F. Wilczek, *Phys. Rev. Lett.* 40, 279 (1978); S. Weinberg, *Phys. Rev. Lett.* 48, 223 (1978). For a recent review of the axion see R.D. Peccei, in *CP Violation*, edited by C. Jarlskog (WSPC, Singapore, 1989). There are two types of axion: one which couples to both quarks and leptons, the DFSZ axion, and one which has no tree-level couplings to leptons, the hadronic axion.
2. See e.g., M.S. Turner, *Phys. Rep.*, in press (1990); or G.G. Raffelt, *ibid*, in press (1991).
3. S. DePanfilis et al., *Phys. Rev. Lett.* 59, 839 (1987); *Phys. Rev. D* 40, 3153 (1989); C. Hagmann, P. Sikivie, N.S. Sullivan, and D.B. Tanner, *Phys. Rev. D (RC)* 42, 1297 (1990).
4. M.S. Turner, *Phys. Rev. Lett.* 59, 2489 (1987).
5. T. Kephart and T. Weiler, *Phys. Rev. Lett.* 58, 171 (1987).
6. P. Massey, C. Gronwall, and C.A. Pilachowski, *Pub. Astron. Soc. Pac.* 102, 1046 (1990).
7. Complete details of our observations, theoretical expectations, astrophysical modeling, and analysis will be given in M.T. Ressel, to be submitted to *Phys. Rev. D* (1991).
8. C.L. Sarazin, *Rev. Mod. Phys.* 58, 1 (1986); A. Dressler, *Astrophys. J.* 223, 765 (1978); A. Dressler, *ibid* 226, 55 (1978); T.C. Beers and J.L. Tonry, *ibid* 300, 557 (1986); L.A. Thompson, *ibid* 306, 384 (1986); S.M. Lea and J.P. Henry, *ibid* 332, 81 (1988); P.E. Boynton, S.J.E. Radford, R.A. Schommer, and S.S. Murray, *ibid* 257, 473 (1982); D.G. Fabricant, S.M. Kent, and M.J. Kurtz, *ibid* 336, 77 (1989); C. Jones and W. Forman, *ibid* 276, C. Jones et al., *ibid* 234, L21 (1979); A. Dressler, *Astrophys. J. Supp.* 42, 565 (1980).
9. J. Binney and S. Tremaine, *Galactic Dynamics* (Princeton Univ. Press, Princeton, 1987), Chs. 1, 2, and 4.
10. We have also considered the approximation, $\rho(r) = \rho_c/(1 + r^2/a^2)$. Since the King model leads to a more conservative limit, we have used it.
11. J. Yang et al., *Astrophys. J.* 281, 493 (1984).
12. The cross-correlation function was computed using the *rvxcor* routine of IRAF. A discussion of this technique and the underlying theory is given by J. Tonry and M. Davis, *Astron. J.* 84, 1511 (1979), and references therein.
13. Previous limits include H.L. Shipman and R. Cowsik, *Astrophys. J. Lett.* 247, L111 (1981); A. de Rujula and S.L. Glashow, *Phys. Rev. Lett.* 45, 942 (1980); R.B. Par-

tridge, to appear in *IAU Symposium 139* (1991). A detailed discussion and comparison of these and our limits will be given elsewhere.

Figure Captions

FIGURE 1: Upper: Spectrum of A2218 at $49''.2$ from the cluster core ($R/a = 0.94$). The spectrum is dominated by the glow of the night sky. Lower: The above spectrum minus a similar spectrum at $4'.96$ from the core ($R/a = 5.33$). The narrow features at 5035\AA and 5350\AA are cosmic-ray hits; note the imperfect night-sky subtractions near strong night sky features.

FIGURE 2: The “on – off” spectrum of A2256 ($R/a = 0.48$ minus $R/a = 2.96$) with a 3.2 eV axion line artificially introduced.

Table 1. Summary of observations and properties of the three clusters.

Cluster	Mass range (eV)	Exposure time (sec)	σ (km s ⁻¹)	a kpc (arcmin)	Inner/Outer Aperture (R/a)	Slit Positions
A1413	3.36–5.95	2700	1230	$400h_{50}^{-1}$ (2.03)	1.11/4.64	3
	3.73–7.58	4500			0.65/2.94	1
A2218	3.44–6.1	2700	1300	$200h_{50}^{-1}$ (0.88)	0.94/5.33	2
	3.82–7.77	4500			0.94/5.33	1
A2256	3.11–5.52	1800	1300	$473h_{50}^{-1}$ (5.0)	0.484/2.96	3

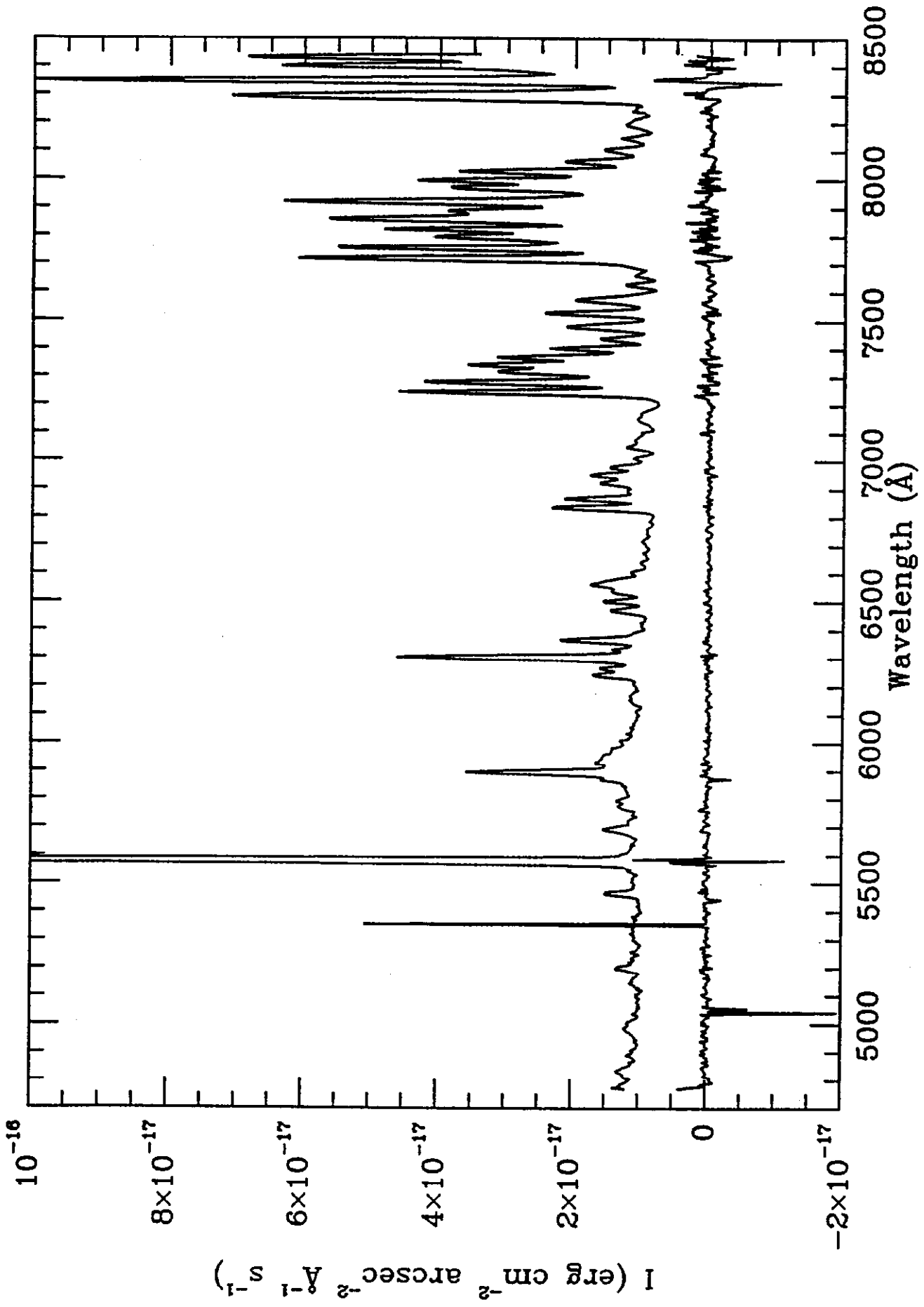


Figure 1

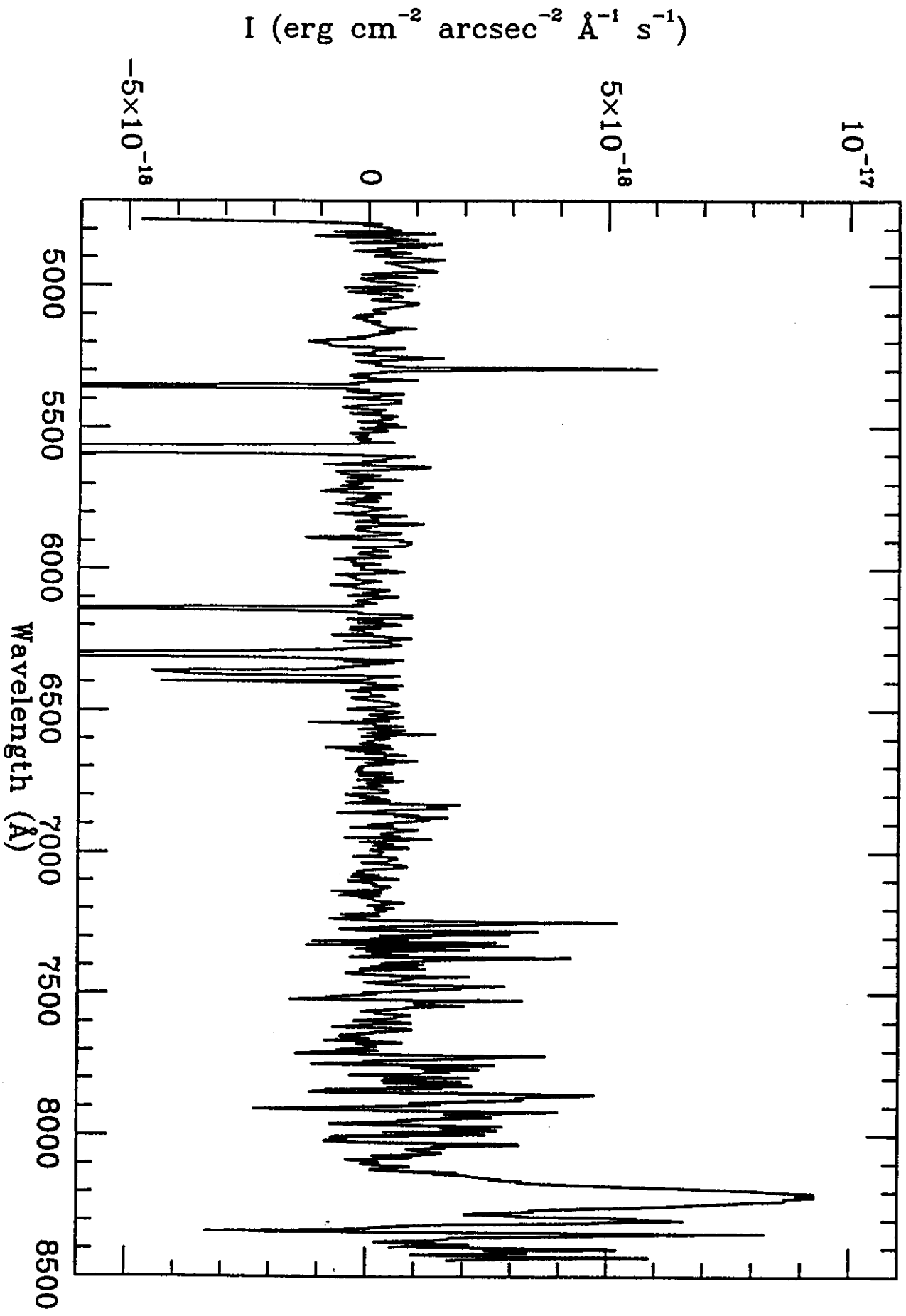


Figure 2